



Voltage controllable superconducting state in the multiterminal superconductor–normal-metal bridge

M. Yu. Levichev, I. Yu. Pashenkin, N. S. Gusev , and D. Yu. Vodolazov ^{*}

Institute for Physics of Microstructures, Russian Academy of Sciences, Nizhny Novgorod, GSP-105, 603950 Russia



(Received 5 January 2021; revised 30 April 2021; accepted 3 May 2021; published 17 May 2021)

We study voltage controllable superconducting state in a multiterminal bridge composed of the dirty superconductor/pure normal metal (SN) bilayer and pure normal metal. In the proposed system small control current I_{ctrl} flows via normal bridge, creates voltage drop V , and modifies the distribution function of electrons in a connected SN bilayer. In the case of a long normal bridge the voltage-induced nonequilibrium effects could be interpreted in terms of increased local electron temperature. In this limit we experimentally find the large sensitivity of critical current I_c of Cu/MoN/Pt-Cu bridge to I_{ctrl} and relatively large current gain which originate from steep dependence of I_c on temperature and large I_c (comparable with theoretical depairing current of the superconducting bridge). In the short normal bridge deviation from equilibrium cannot be described by a simple increase in local temperature, but we also theoretically find large sensitivity of I_c to control current/voltage. In this limit we predict existence at finite V of the so-called in-plane Fulde-Ferrell state with spontaneous currents in the SN bilayer. We argue that its appearance is connected with voltage-induced paramagnetic response in the N layer.

DOI: [10.1103/PhysRevB.103.174507](https://doi.org/10.1103/PhysRevB.103.174507)

I. INTRODUCTION

The idea to control the superconducting properties of superconductors, which are metals, with the help of the electric field or voltage is based on their large sensitivities to the form of the electron distribution function $f(E)$ and the ability to modify $f(E)$ by applied voltage. The origin of the effect could be understood from the equation for the superconducting order parameter Δ ,

$$\Delta = \lambda_{BCS} \int_0^{\hbar\omega_D} R_2(E) f_L(E) dE, \quad (1)$$

where $R_2(E) = Re(\Delta/\sqrt{E^2 - \Delta^2})$ in the simplest case of spatially homogenous superconductor in absence of superconducting current, λ_{BCS} is a coupling constant in Bardeen-Cooper-Schrieffer theory, ω_D is a Debye frequency, and $f_L(E)$ is odd in the energy part of $[1 - 2f(E)]$.

With increasing the bath temperature T the equilibrium Fermi-Dirac distribution $f(E) = 1/[\exp(E/k_B T) + 1]$ changes and $\Delta(T)$ goes down because more states with $E > \Delta(T)$ are occupied by electrons and $f_L(E)$ decreases at low E . At fixed temperature applied voltage V modifies $f(E)$ in a similar way, i.e., $f_L(E)$ decreases with increasing V (for example, see experimental $f(E, V)$ in Ref. [1]), and one can expect voltage controllable modification of superconducting properties. In some cases the effect of V on $f(E)$ could be described via introducing the local electron temperature $T_e(V) \neq T$, for example, in the system with strong electron-electron scattering. But sometimes it cannot be performed, and new effects appear which are connected with nonthermal

form of $f(E, V)$ (the thermal form here is the Fermi-Dirac distribution with $T_e \neq T$).

There are many theoretical and experimental works where the voltage controllable superconducting state was studied in metallic superconductors. For example, in Refs. [2–4] the normal metal-superconductor–normal-metal (NSN) voltage-biased wire was considered. In Ref. [2] there were found that at $eV \sim \Delta$ there is jump to the normal state and in the finite interval of voltages $\Delta/2 < eV < \Delta$ several superconducting states could exist in a voltage-biased “bulk” superconductor. This result could be related with the known transition of the magnetic superconductor to the normal state when magnetic exchange energy $E_{ex} \sim \Delta$ due to the formal analogy between voltage-biased and magnetic superconductors as discussed in Ref. [5]. In Ref. [3] existence of two stable spatially nonuniform states (symmetric and asymmetric against the center of the superconducting part) were predicted for relatively long NSN wire which is a consequence of spatially nonuniform nonequilibrium $f_L(E, V)$. In Ref. [4] the so-called bimodal state was found which may be related to the enhanced stability of superconductivity near the superconductor/normal-metal interface [6]. For the voltage-biased NISIN system there were found several spatially homogenous states at fixed voltage [7] and in some range of the parameters the Fulde-Ferrel-Larkin-Ovchinnikov (FFLO) state was predicted which develops in lateral direction of the NISIN system [5].

Control of the critical current of the SNS (or SINIS) Josephson junction by applying of the voltage (or, alternatively, current) to the additional N lead, attached to the N part of the SNS junction was proposed in Refs. [8–10]. In Refs. [11–13] this effect has been experimentally studied. Recently the control of critical current of Ti and Al bridges with help of the voltage leads has been observed in Refs. [14,15]

^{*}vodolazov@ipmras.ru

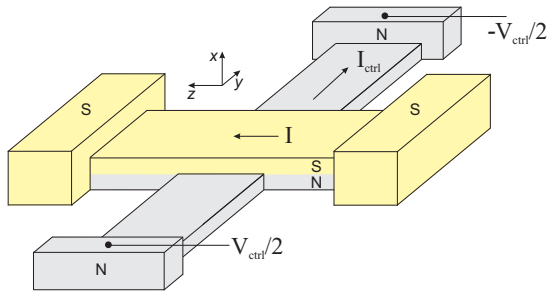


FIG. 1. Sketch of the proposed multiterminal SN-N bridge. The superconducting state of the SN bridge is controlled by voltage drop V_{ctrl} either in the regime of applied voltage or current. S is a thin dirty superconductor with large resistivity in the normal-state (NbN, MoN, MoSi,...), N is a low resistive normal-metal (Au, Cu, and Ag).

where the effect is also connected with modification of $f(E)$ due to applied voltage although in a more complicated manner [16–18] than in previous works.

In our paper we study the current/voltage controllable superconducting state in the multiterminal bridge composed of a superconductor/normal-metal bilayer and normal metal (see Fig. 1), where the superconductor is a highly resistive metal (with large resistivity ρ_S in the normal state) and normal metal has $\rho_N \ll \rho_S$. In the proposed system one may control large critical current (about the depairing current I_{dep} of the S layer) flowing along the SN bridge instead of the much smaller critical current of SNS Josephson junction. In comparison with the superconducting bridge in the SN hybrid with $\rho_S/\rho_N \gg 1$ and thin S and N layers (order of superconducting coherence length) $I_c(T)$ is much steeper in high temperature whereas I_c is much larger at low temperatures [19,20]. These effects come from the substantial superconducting current flowing along the low resistive N layer and the small proximity-induced minigap $\epsilon_g \sim 1/d_N^2$ [21] there, which provides the saturation of $I_c(T)$ at $T \lesssim \epsilon_g/k_B$ [20]. This allows us to expect large sensitivity of I_c even to small deviation from equilibrium caused by applied control current/voltage.

We confirm experimentally these expectations in case of the long normal bridge (Cu) and the long SN bridge (Cu/MoN/Pt) with lengths $L_N, L_{SN} \gg L_{ee}$, where L_{ee} is an inelastic electron-electron scattering length when the deviation from the equilibrium can be described in terms of increased local temperature. For our parameters we find a current gain about six, and we discuss how it could be further improved.

We also study theoretically the limit of the short normal bridge with $L_N \ll L_{ee}$ when nonequilibrium $f_L(E)$ has a non-thermal form in its central part,

$$f_L(E) = \frac{1}{2}(\tanh[(E + eV_{ctrl}/2)/(2k_B T)] + \tanh[(E - eV_{ctrl}/2)/(2k_B T)]). \quad (2)$$

In this limit we also find the large sensitivity of I_c to the control current/voltage, but in addition there is a new effect—the appearance of the in-plane Fulde-Ferrell (FF) state with spontaneous currents flowing along S and N layers in the SN bridge. Previously, the in-plane FFLO state was predicted in the similar nonequilibrium SN system in Ref. [22]. In comparison with that work we show that the FF state appears at finite voltage $V_{ctrl} \sim k_B T_{c0}$ (T_{c0} is a critical temperature of

the superconducting layer), and its origin is connected with voltage-induced paramagnetic response of the N layer which competes with the diamagnetic response of the S layer. Therefore, the situation is similar to the FFLO state in equilibrium SF and SFN hybrid structures [23,24]. And as in the case of the SFN trilayer one needs large ratio $\rho_S/\rho_N \gg 1$ to realize this state in the nonequilibrium SN bilayer.

The structure of the paper is the following. In Sec. II we present our experimental results on the current/voltage controllable superconducting state in the multiterminal SN-N bridge with the long N bridge. In Sec. III we theoretically study the case of the short N bridge and find the range of parameters when the FF state could be realized in the SN bridge and discuss its similarity with the FFLO state in the equilibrium SFN trilayer. In Sec. IV we conclude our results.

II. LONG CONTROL N BRIDGE

At $L_N \gg L_{ee}$ the effect of applied voltage on $f(E)$ could be described via introducing the local electron temperature T_e in the Fermi-Dirac distribution and those spatial distributions along the N bridge satisfy the one-dimensional (when $W_N \ll L_N$) heat conductance equation (see, for example, Eq. (16) in Ref. [25]). In the limit of the short N bridge with L_N smaller than electron-phonon scattering length L_{ep} one may find the simple expression for $T_e(y)$,

$$T_e(y) = \sqrt{T^2 + \alpha V_{ctrl}^2 (1 - y/L_N)y/L_N}, \quad (3)$$

where $\alpha = 3e^2/(\pi^2 k_B^2)$. Equation (3) illustrates that application of voltage/current to the control bridge changes the electron temperature in the SN bridge (which is roughly located at $y = L_N/2$ when $W_{SN} \ll L_N$) and, hence, its critical current.

As we discuss in the Introduction we expect relatively good sensitivity (comparable with that for the SNS junction) and the large current gain in the studied system. To verify it the multiterminal bridges were made using the Cu(30-nm)/MoN(20-nm)/Pt(5-nm) trilayer. The trilayer was grown by magnetron sputtering with a base vacuum level on the order of 1.5×10^{-7} mbars on standard silicon substrates without removing the oxide layer and at room temperature. At first, Cu is deposited in an argon atmosphere at a pressure of 1×10^{-3} mbars. Second, Mo is deposited in an atmosphere of a gas mixture Ar:N₂ = 10:1 at a pressure of 1×10^{-3} mbars, and finally Pt is deposited in an argon atmosphere at a pressure of 1×10^{-3} mbars (the top Pt layer is used for protection purposes). In the next step the multiterminal Cu/MoN/Pt bridges were made with the help of mask free optical lithography. At the final stage the MoN/Pt layers were removed (by plasma chemical etching) in the part of the system to create the normal banks and the bridge. The final configuration is present in Fig. 2(a) where we show the image of one of the multiterminal Cu/MoN/Pt-Cu bridges (the nominal width of Cu/MoN/Pt and Cu bridges is $3 \mu\text{m}$, the length of the Cu/MoN/Pt bridge is $19 \mu\text{m}$, the lengths of the Cu bridge are 5 and $7 \mu\text{m}$, $T_{c0} = 7.8$ K of the MoN film with thickness 20 nm, coherence length $\xi_0 = \sqrt{\hbar D_{MoN}/1.76 k_B T_{c0}} = 4.7$ nm).

In Fig. 2(b) we show current-voltage characteristics of the Cu/MoN/Pt bridge at different values of the control

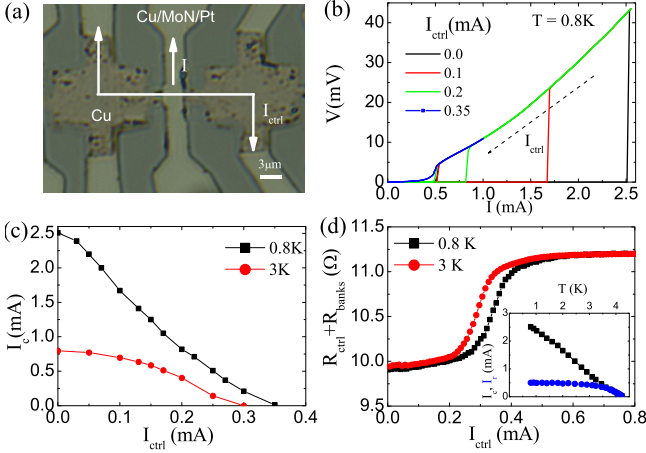


FIG. 2. (a) Image of one of Cu/MoN/Pt-Cu multiterminal bridges. The arrows show the direction of control (I_{ctrl}) and transport (I) currents. The photograph was taken in 4 months after the transport measurements. (b) Current-voltage characteristics of the MoN/Cu/Pt bridge at different values of control current I_{ctrl} in the Cu bridge ($T = 0.8$ K). (c) Dependence of the critical current of the MoN/Cu/Pt bridge on the control current at two temperatures. (d) Dependence of resistance of Cu banks and the bridge on the control current at two temperatures. The inset in panel (d): Temperature dependence of the critical and retrapping currents of the MoN/Cu/Pt bridge ($I_{ctrl} = 0$).

current I_{ctrl} in the Cu bridge measured at $T = 0.8$ K. At $I_{ctrl} > 0.35$ mA the critical current of the SN bridge goes to zero [see Fig. 2(c)] because the part of the normal bridge covered by the MoN layer goes to the normal state [it is seen from Fig. 2(d) where the resistance of normal bridge + normal banks as the function of control current is present]. A similar effect exists at $T = 3$ K [see Figs. 2(c) and 2(d)].

Figure 2(c) demonstrates good sensitivity of the studied system at $T = 0.8$ K—even a small control current may strongly change I_c . A similar sensitivity is typical for SNS junctions [11,13] which also have a steep dependence of I_c on the temperature. On the contrary, in the superconducting bridge only the relatively large applied voltage affects I_c [14,15].

Assuming that the strength of electron-phonon coupling in Au and Cu are close and using electron-phonon scattering time $\tau_{ep}(4.2 \text{ K}) = 1$ ns for Au [11] we find $L_{ep} = \sqrt{D_{Cu}\tau_{ep}} \sim 2.2 \mu\text{m}$ at $T = 4.2$ K ($D_{Cu} \simeq 50 \text{ cm}^2/\text{s}$ according to Ref. [1]) which is comparable with the width and length of our Cu and Cu/MoN/Pt bridges. Therefore, we are neither in the limit of short [when Eq. (3) is valid] nor the long N bridge with $L_N \gg L_{ep}$ [in this case $T_e(L_N/2)$ could be found from the balance between Joule heating and cooling by phonons]. Figure 3 illustrates it where we plot electronic temperature $T_e(I_{ctrl})$ derived from experimental $I_c(T)$, $I_c(I_{ctrl})$, and theoretical $T_e(I_{ctrl})$ in two limits. In calculations we use $V_{ctrl} = I_{ctrl}R_{ctrl}$ where $R_{ctrl} = 6 \Omega$ is estimated from the geometry of Cu banks, measured $R_{ctrl} + R_{banks}$ —see Fig. 2(d), and known sheet resistance $R_{\square} = 1 \Omega$ of the 30-nm-thick Cu layer at 10 K. Electron-phonon coupling strength in Cu is assumed as in Au, leading to above-mentioned τ_{ep} .

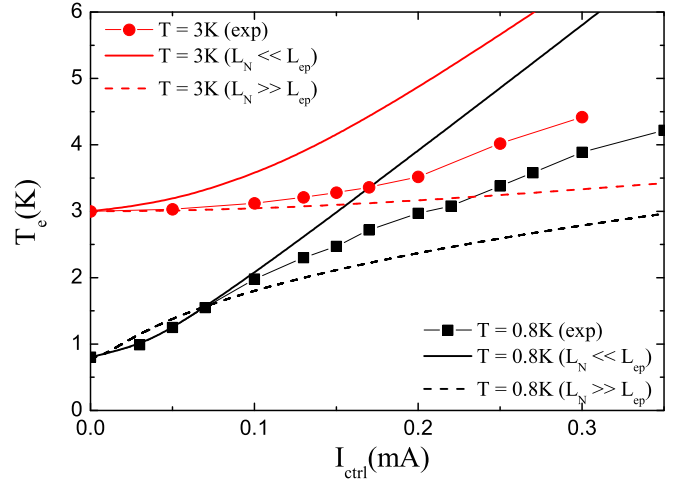


FIG. 3. Dependence of electron temperature T_e in the cross region of the Cu/MoN/Pt and Cu bridges on the control current. Solid symbols are obtained using experimental $I_c(T)$ and $I_c(I_{ctrl})$, whereas the solid and dashed curves follow from the heat conductance equation in the limit of short and long N bridges, respectively.

From Fig. 2 it follows the current gain ~ 6 at $T = 0.8$ K (it is defined as the ratio between I_c at $I_{ctrl} = 0$ and I_{ctrl} which drives I_c to zero) which is larger than the near-unity current gain observed in Ref. [11]. Its relatively large value is connected with the large critical current of the Cu/MoN/Pt bridge (which is about theoretical depairing current $I_{dep}(T = 0) = 11.2$ mA of the MoN bridge with $d_{MoN} = 20$ nm and larger width $w = 5 \mu\text{m}$ [20]) whereas the critical current of the SNS Josephson junction usually is much smaller.

The current gain could be increased either by going to lower temperatures or by optimizing parameters of the structure. Indeed, in Ref. [1] no signs of phonon emission were found for the $5\text{-}\mu\text{m}$ long Cu bridge at 25 mK. Therefore, making the SN-N bridge with $L_N = 5 \mu\text{m}$, $W_N = 200$ nm (and thick normal banks at the ends of the N bridge), $L_{SN} = 5 \mu\text{m}$, $W_{SN} = 1 \mu\text{m}$ (and thick superconducting banks at the ends of the SN bridge) and using parameters of the studied Cu/MoN/Pt-Cu system one can obtain current gain $\gtrsim 60$ [expected critical current $I_c(T = 0) = 1$ mA, expected $I_{ctrl} = 16 \mu\text{A}$, and $V_{ctrl} = 0.4$ mV which drives the SN bridge to the normal state at $T = 100$ mK according to Eq. (3)]. Unfortunately, such a size and temperature is beyond our current abilities.

III. THE FULDE-FERREL STATE IN THE SN-N MULTITERMINAL BRIDGE WITH THE SHORT N BRIDGE

In this section we theoretically study the limit of the short N bridge with length $L_N < L_{ee}$ when the voltage-controlled distribution function in the SN bilayer is not thermal, and it is described by Eq. (2). As we show below it brings a new property, except the possibility to control the critical current as in the long N bridge.

In Refs. [8–10] it was predicted and later experimentally confirmed [12] the sign change in the superconducting current flowing via the diffusive SNS Josephson junction when the distribution function has the form of Eq. (2) in the N part

and the applied voltage is high enough. This result could be interpreted as a transition of the N part of the SNS junction to the paramagnetic state which is a consequence of negative spectral current (or current-carrying density of states) [9,10] in the finite energy range in the N part and the distribution function described by Eq. (2). In the voltage-driven clean SN system the paramagnetic response of the N layer has been predicted recently where its connection with so-called odd-frequency superconductivity has been discussed [26].

The existence of odd-frequency superconductivity was also predicted in the ferromagnetic part of the SF bilayer which has a paramagnetic response [27,28]. At some parameters it may overcome the diamagnetic response of the S layer, and it leads to vanishing of the overall magnetic response, and signals about instability and the appearance of the in-plane Fulde-Ferrell-Larkin-Ovchinnikov state [23]. The appearance of the FFLO state and vanishing of magnetic susceptibility was also discussed in Ref. [29] for the current-driven superconductor with Fermi-surface nesting. Apparently, these two phenomena are correlated in the d -wave superconducting film where the FFLO state with spatially separated paramagnetic and diamagnetic currents flowing in opposite directions across the thickness of the film have been predicted in relatively thin samples [30]. Therefore, one may expect that the nonequilibrium diffusive SN bilayer also may transit to the FFLO state and our aim is to find the conditions when it could be realized. But first we would like to illustrate the transition to the FFLO state in the SFN trilayer having in mind to compare it later with the nonequilibrium SN bilayer.

In Figs. 4(a) and 4(b) we show the calculated superconducting sheet current density $J_z(q_z) = \int j_z(q_z) dx$ flowing along the SFN strip and corresponding free-energy $F_S(q_z)$ when temperature-driven transition to the Fulde-Ferrell state occurs [24] (we do not consider here the Larkin-Ovchinnikov state because it has higher energy than the FF state in the SFN system [31]). Here $q_z = \nabla\varphi_z + (2\pi/\Phi_0)A_z$ is the gauge invariant gradient of the phase of the superconducting order parameter along the SFN trilayer and results are obtained using the Usadel model (details of calculations are present in Ref. [31]). At temperatures $T/T_{c0} = 0.4$ and 0.5 the ground state is homogenous (minimum of free energy is at $q_z = 0$), and the linear magnetic response is diamagnetic because $\partial^2 F_S / \partial q_z^2|_{q_z=0} \sim -\partial J_z / \partial q_z|_{q_z=0} > 0$. At temperatures $T/T_{c0} = 0.1, 0.2$, and 0.3 the ground state is the inhomogeneous one (minimum of free energy is at $q_z = q_{FF}$), but the linear magnetic response is again diamagnetic because $\partial^2 F_S / \partial q_z^2|_{q_z=q_{FF}} > 0$ [32]. At temperature $0.3 < T_{FF}/T_{c0} < 0.4$ there is a transition from the homogenous to the FF state with a change in the sign of $\partial^2 F_S / \partial q_z^2|_{q_z=0}$ (it goes through the zero), and the linear magnetic response vanishes at $T = T_{FF}$. Note that in the case of the relatively large magnetic field (nonlinear regime) transition to the FF state may occur in the globally paramagnetic state (compare the calculated magnetic response of the SFN strip at different magnetic fields and temperatures shown in Fig. 7(a) in Ref. [32]). Vanishing of the linear magnetic response is connected with compensation of the diamagnetic response of the S layer by the paramagnetic response of FN layers.

In Ref. [22] transition to the FFLO state in the nonequilibrium SN bilayer was found theoretically using linearized

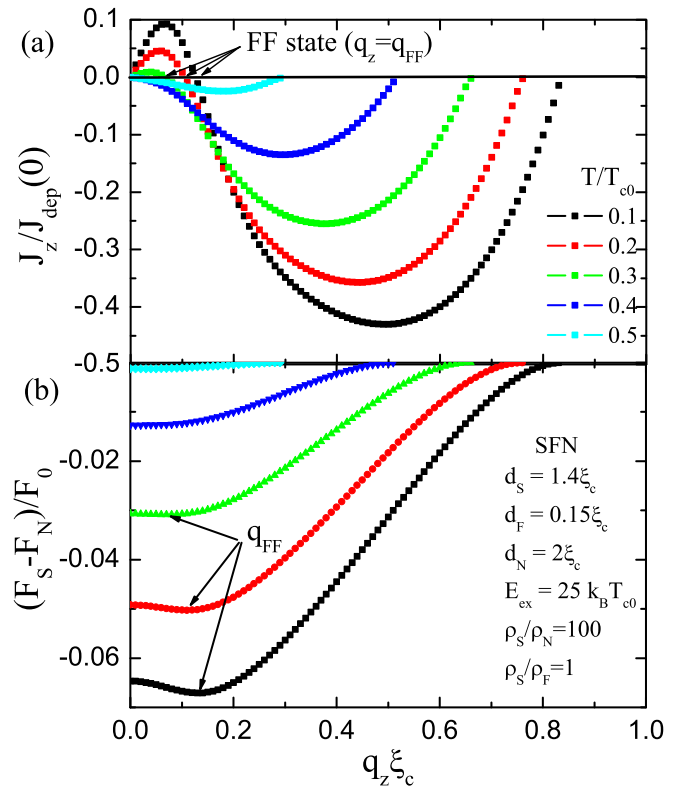


FIG. 4. (a) Dependence of sheet current density J_z flowing along the SFN strip on q_z at different temperatures. In the temperature interval $0.3 < T/T_{c0} < 0.4$ there is a transition to the FF state which is accompanied by the vanishing of the linear diamagnetic (Meissner) response at $T = T_{FF}$. (b) Dependence of the free energy of the SFN strip on q_z at the same temperatures. Parameters of the SFN trilayer are shown in the inset. q_z is normalized in units of $\xi_c = \sqrt{\hbar D_S/k_B T_{c0}}$, sheet current density in units of the depairing sheet current density of the single S layer $J_{dep}(T = 0)$, and the free energy per unit of square in units of $F_0 = \pi N(0)(k_B T_{c0})^2 \xi_c$ (here D_S is a diffusion coefficient, T_{c0} is a critical temperature, $N(0)$ is a one-spin density of states at the Fermi level of the S layer, and E_{ex} is the exchange energy in the F layer).

Usadel equations, however, its relation with the paramagnetic response of the N layer was not established. Here we perform a numerical analysis of nonlinear Usadel equations (see the Appendix) and calculate dependence $J_z(q_z)$ in the SN bridge at different voltage drops along the N bridge (see Fig. 1). We assume that the length of the SN bridge $L_{SN} < L_{ee} < L_{ep}$ and at its ends there is a thick superconductor with gap $\sim 1.76 k_B T_{c0} > eV_{ctrl}$ which prevents heat transfer to superconducting banks. Together with condition $W_{SN} \ll L_N$ it provides us weak coordinate dependence of $f_L(E)$ in the SN bridge. Besides we assume that W_{SN} is larger than $\xi_N = (\hbar D_N/k_B T)^{1/2}$ (coherence length in the normal layer) which is much larger than the superconducting coherence length ξ_0 because $D_N \gg D_S$. This assumption allows us to neglect the influence of the N bridge on the proximity-induced superconductivity in the cross area of the SN and N bridges. Therefore, we take into account the variation of superconducting properties only over the thickness of the SN bridge. In addition we neglect the effect of the superconducting current which flows, in part, of

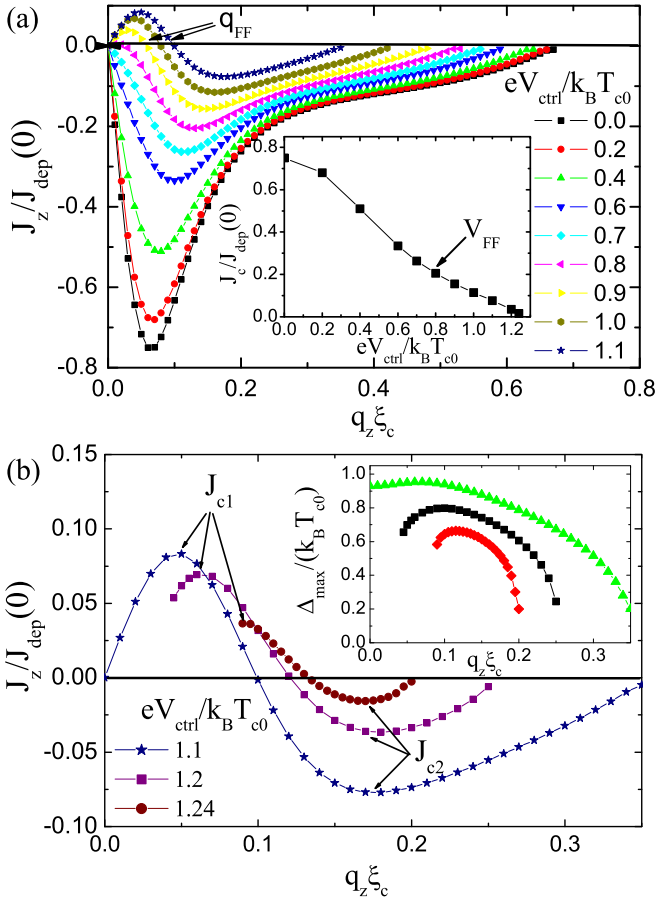


FIG. 5. (a) and (b) Dependence of superconducting sheet current density J_z flowing along the SN strip on q_z at different V_{ctrl} 's. At $eV_{ctrl}/k_B T_{c0} > 0.8$ the branch with $J_z > 0$ and the global paramagnetic response at $q_z = 0$ appear. In the inset of panel (a) we show dependence $J_c(V_{ctrl})$ which is qualitatively similar to $I_c(I_{ctrl})$ present in Fig. 2(c) at $T = 0.8$ K. In the inset of panel (b) we show the dependence of the maximal superconducting order parameter (it is located at the boundary of the S layer with vacuum) on q_z . At $eV_{ctrl}/k_B T_{c0} = 1.2$ and 1.24 there is no homogenous superconducting state with $q_z = 0$. Parameters for the S and N layers are the same as for the SFN trilayer those $J_z(q_z)$ is shown in Fig. 4(a), $T = 0.1T_{c0}$.

the SN bridge due to conversion of the normal control current flowing via the N bridge. In the experiment, to decrease its influence one may vary width and thickness of the N bridge to have smaller I_{ctrl} whereas keeping V_{ctrl} the same. In the narrow SN bridge with $W_{SN} \lesssim \xi_N$ one would expect the absence of (or only partial) conversion of the normal current to the superconducting one as in ordinary superconductors being in contact with normal metal where it converts on the scale of superconducting coherence length at the SN boundary at low temperatures [33].

In Fig. 5 we present calculated $J_z(q_z)$. The voltage drop via the N bridge decreases the critical current [it corresponds to maximal J_z on dependence $J_z(q_z)$] qualitatively in the same manner as it does ordinary heating of electrons discussed in Sec. II [compare the inset in Fig. 5(a) and $I_c(I_{ctrl})$ in Fig. 2(c) at $T = 0.8$ K]. However, at $V_{ctrl} = V_{FF} \sim 0.8k_B T_{c0}$ a new feature appears: J_z changes sign at small q_z , and J_z becomes equal

to zero not only at $q_z = 0$, but also at $q_z = q_{FF}$. This points to the appearance of the in-plane Fulde-Ferrell state in the SN bilayer.

In contrast to the SFN trilayer we cannot use free energy to prove directly that the FF state is more preferable than the homogenous state. Therefore, we lean on the qualitative similarity in the shape of $J_z(q_z)$ for the equilibrium SFN trilayer [see Fig. 4(a)] and the nonequilibrium SN bilayer (see Fig. 5). Indication on the advantage of the FF state comes from Fig. 5(b) where we show $J_z(q_z)$ and $\Delta_{max}(q_z)$ at high voltages [Δ_{max} is the maximal value of $\Delta(x)$ in the S layer]. In the FF state the superconducting order parameter is larger than in the homogenous state—the same effect exists in the SFN trilayer. Besides there is an interesting effect—at the relatively large V_{ctrl} homogenous superconducting state with $q_z = 0$ does not exist—the same effect was found in Ref. [22].

From Fig. 5(a) one can see that at the transition to the FF state dJ_z/dq_z changes the sign at $q_z = 0$. Therefore, as in the case of SF and SFN hybrids the transition to the FF state is accompanied by the vanishing of the linear magnetic (Meissner) response. We find that FF appears at finite $V_{ctrl} = V_{FF}$ with $q_{FF} = 0$ and then q_{FF} increases with the increasing in V_{ctrl} as could be seen from Figs. 5(a) and 5(b). With increasing in the temperature V_{FF} increases whereas V_c (critical voltage which drives the SN bilayer to the normal state) decreases which resembles properties of the magnetic superconductor, which hosts the FFLO state where the role of V is played by the exchange field Ref. [5]. On the contrary, in Ref. [22], it was predicted the existence of the FFLO state with finite q_{FF} at any voltage. The origin for this discrepancy between our results and the results of Ref. [22] is not clear.

In the FF state in the absence of a transport current or a magnetic field there are spontaneous currents flowing in opposite directions across the thickness of the SN bilayer (they also exist in the equilibrium SFN trilayer [24] and in the d -wave thin superconducting film [30]). Their presence is a manifestation of locally diamagnetic (in the S layer), paramagnetic (in the N layer) magnetic response, and finite q_{FF} . In other words coefficient λ^{-2} (which is the inverse square of the London penetration depth for an ordinary superconductor) in relation $j_z \sim -\lambda^{-2} q_z$ has different signs in the S and N layers. For the SN bilayer with a thick S layer there is no transition to the FF state because the voltage-driven paramagnetic response of the N layer cannot compensate the diamagnetic response of the S layer as in the SFN trilayer with the thick S layer [24].

We find that transition to the FF state occurs in a wide range of parameters similar to one for the SFN trilayer [24]. Namely, it occurs at $T \lesssim 0.3T_{c0}$, it may exist at a lower temperature even when $\rho_S/\rho_N = 20$ and for the S layer as thick as $5\xi_c$. The favorite candidates for experimental observation of this state are dirty superconductors, such as NbN, MoN, WSi, etc., with residual resistivity $\rho_S \gtrsim 100 \mu\Omega$ cm, thicknesses $d_S = 1 - 2\xi_c$, and low resistive metals, such as Au, Cu, and Ag with $\rho_N = 2-5 \mu\Omega$ cm and thicknesses $2-4\xi_c$.

In Ref. [1] the two-step electron distribution function [Eq. (2)] was experimentally observed in the center of the Cu bridge with length $1.5 \mu\text{m}$ at $T = 25$ mK. Transition of the Nb/Au/Nb Josephson junction to the π state at $T = 100$ mK with the length of the Au control bridge $1 \mu\text{m}$ was found in Ref. [12]. Both results give approximate length scales and

temperatures when the Fulde-Ferrell state could be observed in the SN-N multiterminal bridge. With the length of the N bridge $L_N = 1.5 \mu\text{m}$ and width $W_N = 100\text{--}200 \text{ nm}$ the width of the SN bridge should be $W_{SN} \lesssim L_N/5 \sim 200 \text{ nm}$ whereas its length L_{SN} is about $1\text{--}1.5 \mu\text{m}$ to avoid thermalization of electrons along the SN bridge.

Spontaneous currents flowing in the nonequilibrium SN bilayer being in the Fulde-Ferrell state create a magnetic field, and it could be checked experimentally by using a superconducting quantum interference device magnetometer. Moreover, one would expect unusual magnetic properties (global paramagnetic response in the Meissner state) and unusual ground states in the absence of a magnetic field (vortex and onionlike ones) connected with the finite size (length and width) of the SN bridge similar to ones predicted for the SFN strip, disk, and square [32,34].

The FF state could be also found from transport measurements. In the regime of applied current only states with $\partial J_z / \partial q_z < 0$ could be realized—these are metastable states [those with $J_z \uparrow \uparrow q_z$ and having critical current J_{c1} in Fig. 5(b)] and ground states ($J_z \uparrow \downarrow q_z$ with critical current J_{c2}) [35]. The transition from the metastable state to the ground state with a change in the current in the range of $-J_{c2} < J < J_{c2}$ is accompanied by a large variation of q_z (it changes value and sign) when $|J|$ exceeds J_{c1} and the appearance of the moving electric domain [36]. Applying ac current at $V_{ctrl} < V_{FF}$ with amplitude $J < J_{c2} = J_c$ (at this control voltage there exist only one critical current) leads to mainly inductive response with the voltage shifted by $\pi/2$ from the current. On the contrary, at $V_{ctrl} > V_{FF}$, the resistive response appears, connected with the change in q_z when the ac current exceeds J_{c1} .

Another way to detect the FF state is to measure current-dependent kinetic inductance $L_k(J)$ of the SN bridge. In an ordinary superconductor $L_k(J) = L_k(-J)$ whereas in the FF superconductor $L_k(J) \neq L_k(-J)$ due to finite $q_z = q_{FF}$ in the ground state. The last property directly follows from the different slopes of $J_z(q_z)$ at $q_z \gtrsim q_{FF}$, $q_z \lesssim q_{FF}$, and relation $L_k^{-1} \sim -\partial J_z / \partial q_z$. For example, $L_k(J = -J_{c1}/2) / L_k(J = J_{c1}/2) \simeq 1.4$ [for $V_{ctrl} = 1.1k_B T_{c0}$ in Fig. 5(a)], and this ratio increases with a further increase in J .

IV. CONCLUSION

We demonstrate experimentally the possibility to control the critical current of the dirty SN hybrid bridge by current/voltage applied to the additional/control normal bridge. We argue that the effect is connected with modification of the electron distribution function in the SN bilayer. In the experiment for our realization of the SN-N multiterminal bridge we find current gain six. Its relatively large value is connected with: (i) the large contribution of proximity-induced superconductivity in the N layer to transport properties of the SN bilayer and (ii) its large sensitivity to the form of the electron distribution function. We argue that the gain could be enhanced by optimization of the geometrical parameters of the SN-N bridge or going to lower temperatures. Besides we theoretically find that proximity-induced superconductivity in the N part of the SN bilayer may have a paramagnetic response at a relatively large voltage drop

and short N bridge and at some parameters it can be larger than the diamagnetic response of the host superconductor. It leads to the appearance of the in-plane Fulde-Ferrell state with properties similar to ones for the hybrid SF or SFN structures, and, apparently, thin d -wave superconducting films and a current-driven superconductor with Fermi-surface nesting.

ACKNOWLEDGMENTS

We acknowledge support from the Foundation for the Advancement of Theoretical Physics and Mathematics ‘‘Basis’’ (Grant No. 18-1-2-64-2) in the part concerned with the theoretical study of the FFLO state in the nonequilibrium SN bilayer, by the Russian State Contract No. 0030-2021-0021 in the part concerned with fabrication of the Cu/MoN/Pt-Cu multiterminal bridge, and by the Russian State Contract No. 0030-2021-0020 in the part concerned with transport measurements.

APPENDIX: MODEL

To calculate superconducting properties across the thickness of the SN bridge being in the voltage-driven nonequilibrium state we use the Usadel equation for anomalous $F = \sin \Theta = N_2 + iR_2$ and normal $G = \cos \Theta = N_1 + iR_1$ Green’s functions,

$$\hbar D \frac{d\Theta^2}{dx} + \left(2iE - \frac{D}{\hbar} q_z^2 \cos \Theta \right) \sin \Theta + 2\Delta \cos \Theta = 0, \quad (\text{A1})$$

where D is a diffusion coefficient ($D = D_S$ in the superconducting layer and $D = D_N$ in the normal layer), $q_z = \nabla \varphi_z + (2\pi/\Phi_0)A_z$ (φ is a phase of the order parameter, A is a vector potential) takes into account nonzero velocity of superconducting electrons $v_s \sim q_z$ in the direction parallel to layers (z direction in our case), and $\Delta(x)$ is a magnitude of superconducting order parameter which has to be found in the superconducting layer via self-consistency equation,

$$\Delta = \lambda_{BCS} \int_0^{\hbar\omega_D} R_2 f_L(E) dE, \quad (\text{A2})$$

where

$$f_L(E) = \frac{1}{2} (\tanh[(E + eV_{ctrl}/2)/(2k_B T)] + \tanh[(E - eV_{ctrl}/2)/(2k_B T)]). \quad (\text{A3})$$

To calculate the superconducting sheet current density we use the following expression:

$$J_z = \frac{q_z}{e\hbar} \int_0^{d_S+d_N} \frac{1}{\rho} \int_0^\infty 2N_2 R_2 f_L(E) dE dx, \quad (\text{A4})$$

where ρ is the normal-state resistivity of the S and N layers. We consider a thin bilayer with the thickness of superconducting layer $d_S \ll \lambda_L$ (λ_L is the London penetration depth in the S layer) and thickness of normal layer d_N less than characteristic penetration depth of the magnetic field in the N layer. It allows us to neglect the effect of the current-induced magnetic field on the current distribution in the SN strip.

At the SN interface ($x = d_N$) we use the following boundary condition:

$$D_N \frac{d\Theta}{dx} \Big|_{x=d_N-0} = D_S \frac{d\Theta}{dx} \Big|_{x=d_N+0}, \quad (\text{A5})$$

and continuity of Θ : $\Theta(x = d_N - 0) = \Theta(x = d_N + 0)$ (we assume the transparent interface between S and N layers), whereas at the boundary with vacuum ($x = 0, d_N + d_S$): $d\Theta/dx = 0$.

Equations (A1) and (A2) are solved numerically by using an iteration procedure. For initial distribution $\Delta(x) = \text{const}$ we solve Eq. (A1) in the energy interval $0 < E < \hbar\omega_D$ (we take $\hbar\omega_D = 40k_B T_{c0}$). In the numerical procedure we use the Newton method combined with the tridiagonal matrix algorithm. The found solution $\Theta(x)$ is inserted in Eq. (A2) to find $\Delta(x)$, and then iterations repeat until the relative change in

$\Delta(x)$ between two iterations does not exceed 10^{-8} . The length is normalized in units of $\xi_c = \sqrt{\hbar D_S / k_B T_{c0}}$, energy is in units of $k_B T_{c0}$, and current is in units of depairing current of the single S layer with the thickness d_S . The typical step grid in the S and N layers is $\delta x = 0.05\xi_c$. The BSC constant in Eq. (A2) is expressed via $\hbar\omega_D$ and T_{c0} using the following expression:

$$\lambda_{BCS} = \int_0^{\hbar\omega_D} \frac{\tanh(E/2k_B T_{c0})}{E} dE, \quad (\text{A6})$$

which follows from Eq. (A2) when $\Delta \rightarrow 0$, $R_2/\Delta \rightarrow 1/E$, and $V_{crrl} = 0$.

To decrease the number of free parameters we assume that the density of states in the S and N layers is the same and the ratio of resistivities is equal to the inverse ratio of diffusion constants or mean free paths $\rho_S/\rho_N = D_N/D_S = \ell_N/\ell_S$.

-
- [1] H. Pothier, S. Gueron, N. O. Birge, D. Esteve, and M. H. Devoret, Energy Distribution Function of Quasiparticles in Mesoscopic Wires, *Phys. Rev. Lett.* **79**, 3490 (1997).
- [2] R. S. Keizer, M. G. Flokstra, J. Aarts, and T. M. Klapwijk, Critical Voltage in Superconductors, *Phys. Rev. Lett.* **96**, 147002 (2006).
- [3] D. Y. Vodolazov and F. M. Peeters, Symmetric and asymmetric states in a mesoscopic superconducting wire in the voltage-driven regime, *Phys. Rev. B* **75**, 104515 (2007) (see also extended version [arXiv:0611315](https://arxiv.org/abs/0611315)).
- [4] N. Vercruyssen, T. G. A. Verhagen, M. G. Flokstra, J. P. Pekola, and T. M. Klapwijk, Evanescent states and nonequilibrium in driven superconducting nanowires, *Phys. Rev. B* **85**, 224503 (2012).
- [5] A. Moor, A. F. Volkov, and K. B. Efetov, Inhomogeneous state in nonequilibrium superconductor/normal-metal tunnel structures: A Larkin-Ovchinnikov-Fulde-Ferrell-like phase for nonmagnetic systems, *Phys. Rev. B* **80**, 054516 (2009).
- [6] B. I. Ivlev and N. B. Kopnin, Electric currents and resistive states in thin superconductors, *Adv. Phys.* **33**, 47 (1984).
- [7] I. Snyman and Y. V. Nazarov, Bistability in voltage-biased normal-metal/insulator/superconductor/insulator/normal-metal structures, *Phys. Rev. B* **79**, 014510 (2009).
- [8] A. F. Volkov, New Phenomena in Josephson SINIS Junctions, *Phys. Rev. Lett.* **74**, 4730 (1995).
- [9] S. K. Yip, Energy-resolved supercurrent between two superconductors, *Phys. Rev. B* **58**, 5803 (1998).
- [10] F. K. Wilhelm, G. Schon, and A. D. Zaikin, Mesoscopic Superconducting–Normal Metal–Superconducting Transistor, *Phys. Rev. Lett.* **81**, 1682 (1998).
- [11] A. F. Morpurgo, T. M. Klapwijk, and B. J. van Wees, Hot electron tunable supercurrent, *Appl. Phys. Lett.* **72**, 966 (1998).
- [12] J. J. A. Baselmans, A. F. Morpurgo, B. J. van Wees, and T. M. Klapwijk, Reversing the direction of the supercurrent in a controllable Josephson junction, *Nature (London)* **397**, 43 (1999).
- [13] Z. Xu, S. Chen, W. Tian, Z. Qi, W. Yue, H. Du, H. Sun, C. Zhang, J. Wu, S. Dong, Y.-L. Wang, W. Xu, B. Jin, J. Chen, G. Sun, D. Koelle, R. Kleiner, H. Wang, and P. Wu, Vertical Nb/TiO_x/Nb Josephson Junctions Controlled by In-Plane Hot-Electron Injection, *Phys. Rev. Appl.* **14**, 024008 (2020).
- [14] G. De Simoni, F. Paolucci, P. Solinas, E. Strambini, and F. Giazotto, Metallic supercurrent field-effect transistor, *Nat. Nanotechnol.* **13**, 802 (2018).
- [15] F. Paolucci, G. De Simoni, Paolo Solinas, E. Strambini, N. Ligato, P. Virtanen, A. Braggio, and F. Giazotto, Magnetotransport Experiments on Fully Metallic Superconducting Dayem-Bridge Field-Effect Transistors, *Phys. Rev. Appl.* **11**, 024061 (2019).
- [16] I. Golokolenov, A. Guthrie, S. Kafanov, Y. Pashkin, and V. Tsepelin, On the origin of the controversial electrostatic field effect in superconductors, [arXiv:2009.00683](https://arxiv.org/abs/2009.00683) [Nat. Commun. (to be published)].
- [17] L. D. Alegria, C. G. L. Böttcher, A. K. Saydjari, A. T. Pierce, S. H. Lee, S. P. Harvey, U. Vool, and A. Yacoby, High-energy quasiparticle injection into mesoscopic superconductors, *Nat. Nanotechnol.* **16**, 404 (2021).
- [18] M. F. Ritter, A. Fuhrer, D. Z. Haxell, S. Hart, P. Gumann, H. Riel, and F. Nichele, A superconducting switch actuated by injection of high-energy electrons, *Nat. Commun.* **12**, 1266 (2021).
- [19] D. Y. Vodolazov, A. Y. Aladyshkin, E. E. Pestov, S. N. Vdovichev, S. S. Ustavshikov, M. Y. Levichev, A. V. Putilov, P. A. Yunin, A. I. El'kina, N. N. Bukharov, and A. M. Klushin, Peculiar superconducting properties of a thin film superconductor-normal metal bilayer with large ratio of resistivities, *Supercond. Sci. Technol.* **31**, 115004 (2018).
- [20] S. S. Ustavshikov, Y. N. Nozdrin, M. Y. Levichev, A. V. Okomel'kov, I. Y. Pashenkin, P. A. Yunin, A. M. Klushin, and D. Y. Vodolazov, Photoresponse of current-biased superconductor/normal metal strip with large ratio of resistivities, *J. Phys. D: Appl. Phys.* **53**, 395301 (2020).
- [21] W. Belzig, C. Bruder, and G. Schon, Local density of states in a dirty normal metal connected to a superconductor, *Phys. Rev. B* **54**, 9443 (1996).
- [22] I. V. Bobkova and A. M. Bobkov, In-plane Fulde-Ferrel-Larkin-Ovchinnikov instability in a superconductor–normal metal

- bilayer system under nonequilibrium quasiparticle distribution, *Phys. Rev. B* **88**, 174502 (2013).
- [23] S. Mironov, A. Mel'nikov, and A. Buzdin, Vanishing Meissner effect as a Hallmark of in-Plane Fulde-Ferrell-Larkin-Ovchinnikov Instability in Superconductor-Ferromagnet Layered Systems, *Phys. Rev. Lett.* **109**, 237002 (2012).
- [24] S. V. Mironov, D. Vodolazov, Y. Yerin, A. V. Samokhvalov, A. S. Melnikov, and A. Buzdin, Temperature Controlled Fulde-Ferrell-Larkin-Ovchinnikov Instability in Superconductor-Ferromagnet Hybrids, *Phys. Rev. Lett.* **121**, 077002 (2018).
- [25] K. E. Nagaev, Influence of electron-electron scattering on shot noise in diffusive contacts, *Phys. Rev. B* **52**, 4740 (1995).
- [26] J. A. Ouassou, W. Belzig, and J. Linder, Prediction of a Paramagnetic Meissner Effect in Voltage-Biased Superconductor-Normal-Metal Bilayers, *Phys. Rev. Lett.* **124**, 047001 (2020).
- [27] F. S. Bergeret, A. F. Volkov, and K. B. Efetov, Josephson current in superconductor-ferromagnet structures with a nonhomogeneous magnetization, *Phys. Rev. B* **64**, 134506 (2001).
- [28] A. F. Volkov, F. S. Bergeret, and K. B. Efetov, Odd Triplet Superconductivity in Superconductor-Ferromagnet Multilayered Structures, *Phys. Rev. Lett.* **90**, 117006 (2003).
- [29] H. Doh, M. Song, and H.-Y. Kee, Novel Route to a Finite Center-of-Mass Momentum Pairing State for Superconductors: A Current-Driven Fulde-Ferrell-Larkin-Ovchinnikov State, *Phys. Rev. Lett.* **97**, 257001 (2006).
- [30] A. B. Vorontsov, Broken Translational and Time-Reversal Symmetry in Unconventional Superconducting Films, *Phys. Rev. Lett.* **102**, 177001 (2009).
- [31] P. M. Marychev and D. Y. Vodolazov, Tuning the in-plane Fulde-Ferrell-Larkin-Ovchinnikov state in a superconductor/ferromagnet/normal-metal hybrid structure by current or magnetic field, *Phys. Rev. B* **98**, 214510 (2018).
- [32] P. M. Marychev, V. D. Plastovets, and D. Y. Vodolazov, Magnetic field induced global paramagnetic response in Fulde-Ferrell superconducting strip, *Phys. Rev. B* **102**, 054519 (2020).
- [33] S. N. Artemenko and A. F. Volkov, Electric fields and collective oscillations in superconductors, *Sov. Phys. Usp.* **22**, 295 (1979).
- [34] V. D. Plastovets and D. Y. Vodolazov, Paramagnetic Meissner, vortex, and onion-like ground states in a finite-size Fulde-Ferrell superconductor, *Phys. Rev. B* **101**, 184513 (2020).
- [35] K. V. Samokhin and B. P. Truong, Current-carrying states in Fulde-Ferrell-Larkin-Ovchinnikov superconductors, *Phys. Rev. B* **96**, 214501 (2017).
- [36] V. D. Plastovets and D. Y. Vodolazov, Dynamics of Domain Walls in a Fulde-Ferrell Superconductor, *JETP Lett.* **109**, 729 (2019).